

Luminescence properties of *m*-terphenyl-based Eu^{3+} and Nd^{3+} complexes: visible and near-infrared emission

2
PERKIN

Manon P. Oude Wolbers,^a Frank C. J. M. van Veggel,^{*,a}
Johannes W. Hofstraat,^b Frank A. J. Geurts^b and David N. Reinhoudt^{*,a}

^a Department of Supramolecular Chemistry and Technology, University of Twente,
PO Box 217, 7500 AE Enschede, The Netherlands

^b Akzo Nobel Central Research b.v., PO Box 9300, 6800 SB Arnhem, The Netherlands

Two novel *m*-terphenyl-based organic ligands (**2** and **3**) have been synthesized. Photophysical studies show that the ligands form stable complexes with Eu^{3+} , since typical Eu^{3+} luminescence is observed upon excitation of the ligand. The acyclic complex $2 \cdot \text{Eu}^{3+}$ shows relatively long lifetimes in methanol (e.g. $\tau = 0.72$ ms in CH_3OH). The acyclic ligand **2** allows the additional coordination of two solvent molecules and their high-energy vibrational modes form the main quenching pathway for the Eu^{3+} luminescence. In comparison with $1 \cdot \text{Eu}^{3+}$, the more rigid dioxolane-containing complex $3 \cdot \text{Eu}^{3+}$ provides an additional donor atom, which reduces the solvent coordination of $3 \cdot \text{Eu}^{3+}$ ($\tau_{3 \cdot \text{Eu}^{3+}} = 1.42$ ms compared to $\tau_{1 \cdot \text{Eu}^{3+}} = 0.75$ ms in CH_3OH). The high-energy vibrational modes of the organic ligand **3** are the most important quenchers. Typical near-infrared Nd^{3+} emission at 1060 and 1350 nm resulting from $3 \cdot \text{Nd}^{3+}$ has been observed. Quenching by the solvent is still operative for $3 \cdot \text{Nd}^{3+}$, because of the larger ionic radius of the Nd^{3+} ion.

Introduction

Recently, we have published the luminescence properties of Eu^{3+} complexes of a series of novel preorganized hemispherand-based polydentates, such as **1**.¹ We have shown that this ligand system reduces the solvent coordination to only 1 ± 0.5 O–H oscillator in the first coordination sphere of the Eu^{3+} ion. We have determined the rate constants for quenching by several high-energy vibrational modes surrounding the Eu^{3+} ion by systematic deuteration of the ligand system. This leads to the unambiguous conclusion that quenching by the encapsulating ligand **1** is of the same order of magnitude as quenching

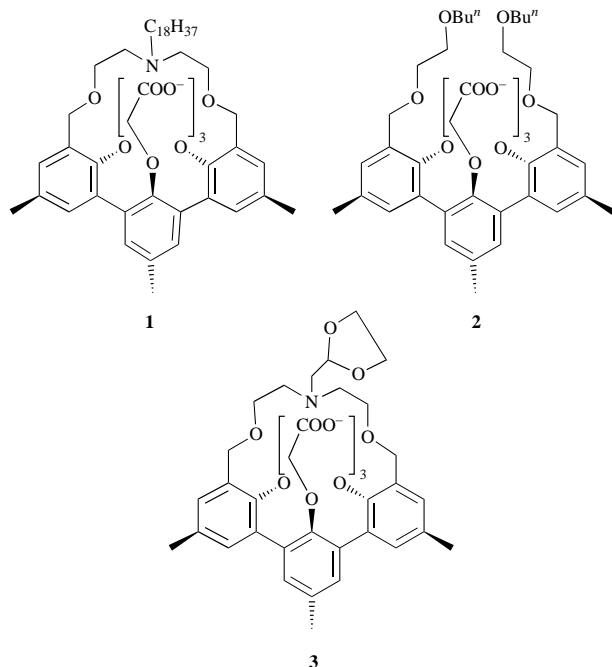
The work described in this paper is part of our investigation of the application of organic lanthanide ion complexes as optical amplifiers in polymer-based waveguides and of the delayed luminescence that is applicable in immunoassays.⁴ In general long-lived luminescence in the near-infrared (NIR) region of the electromagnetic spectrum is useful for application in optical amplifiers, provided that the long luminescence lifetimes do not lead to energy-consuming side processes. In this paper, we use Eu^{3+} as a model to study the effects of organic ligands on luminescence properties, because Eu^{3+} luminescence can be easily measured and the luminescence properties of Eu^{3+} complexes are well documented.⁵ In order to study the effect of the flexibility of the encapsulating ligand, a novel acyclic *m*-terphenyl-based ligand **2** was synthesized. This ligand contains *n*-butoxyethoxy groups at the benzylic positions and provides an additional donor atom in a more flexible structure compared to **1**. Since we have found that the shielding properties of the highly preorganized ligand **1** were quite effective,¹ an additional functional group was introduced at the nitrogen atom in the azacrown bridge, leading to the dioxolane-containing ligand **3**. It is expected that the lanthanide ion is shielded even more effectively from the solvent molecules when complexed by this preorganized macrocyclic ligand. In addition, the luminescence properties of Nd^{3+} complexes are interesting because the emission band at 1350 nm is compatible with the currently operative telecommunication system.⁶ In this paper, the synthesis, photophysical studies and molecular modelling of the complexes $2 \cdot \text{Eu}^{3+}$, $3 \cdot \text{Eu}^{3+}$ and $3 \cdot \text{Nd}^{3+}$ are reported.

Experimental

Synthesis

Melting points were determined with a Reichert melting point apparatus and are uncorrected. ¹H NMR and ¹³C NMR spectra were recorded in CDCl_3 (unless otherwise stated) with Me_4Si as internal standard on a Bruker AC 250 spectrometer. *J* values are given in Hz. Mass spectra were recorded with a Finnigan MAT 90 spectrometer using *m*-NBA (3-nitrobenzyl alcohol) as a matrix, unless otherwise stated. IR spectra were obtained using a Biorad 3200 or a Nicolet 55XC FT-IR spectrophotometer.

by one coordinating solvent molecule. Recently, Dickins² and Hemmilä³ and their co-workers also reported a significant increase in luminescence lifetime upon ligand deuteration.



Elemental analysis † was performed using a Carlo Erba EA1106. The Eu³⁺ content was determined by destroying the ligand in the presence of concentrated nitric acid and concentrated perchloric acid. The remaining acids were evaporated, the salts dissolved in Q₂ water, followed by the addition of an acetate buffer to keep the pH at 5–5.5, and a drop of pyridine was added. After heating to 60 °C, a titration with an aqueous solution of 0.01 M EDTA (ethylenediamine tetraacetate) was carried out using xylenol orange as an indicator. CH₂Cl₂ was distilled from CaCl₂, and THF from Na–benzophenone prior to use. CH₃CN and MeOH were dried over molecular sieves (3 Å) for at least 3 days. NaH was a 55% dispersion in mineral oil and was used as such. The complex Et₃N·HCOOH was obtained prior to use by distillation under reduced pressure (17 mmHg) of an equimolar mixture of formic acid and Et₃N at 70 °C. All other chemicals were of reagent grade and were used without further purification. Column chromatography was performed using silica gel 60 (particle size: 0.040–0.063 mm, 2230–400 mesh) from Merck. All reactions were carried out under an argon atmosphere. The different rings of the terphenyl moiety will be expressed by 'i' and 'o' for the inner ring and the outer rings, respectively.

2,6-Bis[3-(*n*-butoxyethoxymethyl)-5-methyl-2-(prop-2-enyloxy)phenyl]-4-methyl-1-(prop-2-enyloxy)benzene (5). A solution of dibromide **4** (2.02 g, 3.22 mmol) in THF (10 ml) and a solution of *n*-butoxyethanol (0.93 g, 7.11 mmol) in THF (10 ml) were added dropwise to a refluxing suspension of NaH (0.56 g, 13 mmol) in THF (30 ml). After the addition was complete the reaction mixture was refluxed for an additional hour followed by cooling to room temperature and careful addition of water (5 ml) to destroy the remaining NaH. Subsequently, the solvent was evaporated and EtOAc (50 ml) was added to the residue. The organic layer was washed twice with brine, separated and dried with MgSO₄. The organic layer was evaporated to give compound **5** as a dark yellow oil in quantitative yield, which was pure according to the ¹H NMR spectrum. δ_H 7.23 (d, 2 H, *J* 2.0, ArH^o), 7.17 (s, 2 H, ArHⁱ), 7.14 (d, 2 H, *J* 2.0, ArH^o), 5.9–5.7 (m, 2 H, CH=CH^o), 5.5–5.3 (m, 1 H, CH=CHⁱ), 5.2–5.0 (m, 4 H, CH=CH^o), 4.9–4.7 (m, 2 H, CH=CHⁱ), 4.64 (s, 4 H, ArCH₂O), 4.08 (d, 4 H, *J* 5.6, ArOCH₂), 3.89 (d, 2 H, *J* 5.6, ArOCH₂), 3.7–3.6 (m, 8 H, OCH₂), 3.47 (t, 4 H, *J* 6.6, OCH₂), 2.32 (s, 3 H, ArCH₃), 2.31 (s, 6 H, ArCH₃), 1.6–1.5 (m, 4 H, CH₂), 1.5–1.2 (m, 4 H, CH₂), 0.90 (t, 6 H, *J* 7.3, CH₃); δ_C 152.5 (s, ArC–O^o), 152.2 (s, ArC–Oⁱ), 134.2–129.4 (ArC and CH=CH^o), 116.9 (t, CH=CH^o), 116.4 (t, CH=CHⁱ), 74.4 (t, ArO–CH₂), 73.6 (t, ArO–CH₂), 71.2, 70.2 (t, OCH₂), 69.9 (t, Ar–CH₂O), 68.5 (t, OCH₂), 31.8, 29.7 (t, CH₂), 20.8 (q, Ar–CH₃), 20.7 (q, Ar–CH₃), 19.3 (t, CH₂), 14.1, 13.9 (q, CH₃); *m/z* (FABMS) 700.8 [M⁺, calc. for C₄₄H₆₀O₇: 700.4].

2,6-Bis[3-(*n*-butoxyethoxymethyl)-2-hydroxy-5-methylphenyl]-4-methylphenol (6). A mixture of **5** (2.34 g, 3.34 mmol), Pd(PPh₃)₄ (0.27 g, 0.23 mmol), Et₃N·HCOOH (1.48 g, 10.0 mmol) in EtOH (30 ml) and water (6 ml) was refluxed for 1 h. After cooling the resulting mixture to room temperature, the organic solvent was evaporated and the remaining mixture was dissolved in EtOAc (50 ml) and washed with brine (2 × 50 ml). The product was dried over MgSO₄ and **6** was obtained in 86% yield as a slightly yellow oil. The product, which was pure according to ¹H NMR spectroscopy, was used without further purification. δ_H 7.14 (s, 2 H, ArHⁱ), 7.13 (d, 2 H, *J* 2.0, ArH^o), 7.02 (d, 2 H, *J* 2.0, ArH^o), 4.75 (br s, 4 H, ArCH₂O), 3.8–3.6 (m, 4 H, OCH₂), 3.7–3.5 (m, 4 H, OCH₂), 3.45 (t, 4 H, *J* 6.6, OCH₂), 2.36 (s, 3 H, ArCH₃), 2.33 (s, 6 H, ArCH₃), 1.6–1.4 (m, 4 H, CH₂), 1.4–1.2 (m, 4 H, CH₂), 0.86 (t, 6 H, *J* 7.3, CH₃); δ_C 149.6 (s, ArC–O^o), 147.7 (s, ArC–Oⁱ), 130.2–126.4 (ArC), 71.0 (t, Ar–CH₂O), 70.8, 69.3 (t, OCH₂), 31.8 (t, CH₂),

20.4 (q, Ar–CH₃), 20.3 (q, Ar–CH₃), 19.6 (t, CH₂), 13.6 (q, CH₃); *m/z* (FABMS) 579.5 [(M–H)[–], calc. for C₃₅H₄₇O₇: 579.3].

2,6-Bis[3-(*n*-butoxyethoxymethyl)-2-(ethoxycarbonylmethoxy)-5-methylphenyl]-4-methyl-1-(ethoxycarbonylmethoxy)benzene (7). A mixture of triol **6** (2.40 g, 4.13 mmol), K₂CO₃ (2.28 g, 16.5 mmol) and ethyl bromoacetate (1.83 ml, 16.5 mmol) in CH₃CN (50 ml) was refluxed overnight. After cooling to room temperature, the salts were filtered off and the filtrate was concentrated to dryness. CH₂Cl₂ (50 ml) was added to the residue and the organic solution was washed with brine, dried with MgSO₄ and concentrated to dryness. The product was purified by column chromatography (EtOAc:*n*-hexane = 1:2) and obtained as a colorless oil in 82% yield. δ_H 7.17 (d, 2 H, *J* 2.0, ArH^o), 7.2–7.1 (m, 4 H, ArHⁱ and ArH^o), 4.67 (br s, 4 H, ArCH₂O), 4.25 (br s, 4 H, ArOCH₂), 4.12 (br s, 2 H, ArO–CH₂), 4.11 (q, 4 H, *J* 7.1, OCH₂CH₃), 3.94 (q, 2 H, *J* 7.1, OCH₂CH₃), 3.7–3.6 (m, 4 H, OCH₂), 3.6–3.5 (m, 4 H, OCH₂), 3.45 (t, 4 H, *J* 6.6, OCH₂), 2.35 (s, 9 H, ArCH₃ⁱ and ArCH₃^o), 1.6–1.4 (m, 4 H, CH₂), 1.4–1.2 (m, 4 H, CH₂), 1.20 (t, 6 H, *J* 7.1, OCH₂CH₃), 1.07 (t, 3 H, *J* 7.1, OCH₂CH₃), 0.90 (t, 6 H, *J* 7.4, CH₃); δ_C 169.2 (s, C=O^o), 168.8 (s, C=Oⁱ), 152.2 (s, ArC–O^o), 151.7 (s, ArC–Oⁱ), 135.9–129.2 (ArC), 71.2 (t, Ar–CH₂O), 70.3 (t, ArO–CH₂), 70.0 (t, ArO–CH₂), 69.9, 68.8 (t, OCH₂), 60.9 (t, OCH₂CH₃), 60.7 (t, OCH₂CH₃), 32.0 (t, OCH₂), 21.0 (q, Ar–CH₃), 20.8 (q, Ar–CH₃), 19.4 (t, CH₂), 14.1, 13.9 (q, OCH₂CH₃); *m/z* (FABMS) 861.1 [(M + Na)⁺, calc. for C₄₇H₆₆O₁₃Na: 861.5].

2,6-Bis[3-(*n*-butoxyethoxymethyl)-2-(hydroxycarbonylmethoxy)-5-methylphenyl]-4-methyl-1-(hydroxycarbonylmethoxy)benzene (8). Triester **7** (1.79 g, 2.14 mmol) was dissolved in MeOH (15 ml) after which a solution of NaOMe [Na (0.26 g, 10.7 mmol) and 5 ml of MeOH] was added, followed by the addition of water (0.23 ml, 12.8 mmol). According to TLC (MeOH:CH₂Cl₂ = 1:9), the reaction was completed after stirring for 1 week. Subsequently, EtOAc was added and then the reaction mixture was acidified with 1 M HCl in water to pH < 1. The solvent was evaporated, after which EtOAc (20 ml) was added and the solution was subsequently washed with water (2×) and brine (1×). The solution was concentrated and product **8** was dried by extracting twice with toluene (20 ml). The product was obtained in almost quantitative yield as a slightly yellow oil which was pure according to ¹H NMR spectroscopy. δ_H 7.98 (br s, 3 H, OH), 7.2–7.0 (m, 6 H, ArHⁱ and ArH^o), 4.62 (br s, 4 H, ArCH₂O), 4.17 (br s, 4 H, ArOCH₂), 4.00 (br s, 2 H, ArOCH₂), 3.7–3.6 (m, 4 H, OCH₂), 3.6–3.5 (m, 4 H, OCH₂), 3.43 (t, 4 H, *J* 6.8, CH₂), 2.36 (s, 3 H, ArCH₃), 2.31 (s, 6 H, ArCH₃), 1.6–1.5 (m, 4 H, CH₂), 1.4–1.2 (m, 4 H, CH₂), 0.86 (t, 6 H, *J* 7.2, CH₃); δ_C 170.4 (s, C=O^o), 170.1 (s, C=Oⁱ), 152.3 (s, ArC–O^o and ArC–Oⁱ), 134.2–129.5 (ArC), 71.3 (t, Ar–CH₂O), 70.5 (t, ArO–CH₂), 69.8 (t, ArO–CH₂), 69.4 (t, OCH₂), 31.4 (t, CH₂), 20.7 (q, Ar–CH₃ⁱ and Ar–CH₃^o), 19.2 (t, CH₂), 13.9 (q, CH₃); ν_{max}(KBr)/cm^{–1} 1750 (C=O); *m/z* (FABMS) 777.0 [(M + Na)⁺, calc. for C₄₁H₅₄O₁₃Na: 777.4].

2,6-Bis[3-(*n*-butoxyethoxymethyl)-2-(carboxylatomethoxy)-5-methylphenyl]-4-methyl-1-(carboxylatomethoxy)benzene europium(III) (2·Eu³⁺). Triacid **8** (0.10 g, 0.13 mmol) was dissolved in methanol (2 ml), after which three equivalents of Et₃N (55 μl, 0.40 mmol) were added using a microsyringe. Subsequently, a solution of EuCl₃·6H₂O (50 mg, 0.14 mmol) in methanol (1 ml) was added in one portion. The reaction mixture was stirred overnight, followed by evaporation of the organic solvent, and subsequent addition of water (2 ml). The complex was extracted with CH₂Cl₂ and the organic layer was dried over MgSO₄. Complex **2·Eu³⁺** was obtained as a slightly yellow solid in almost quantitative yield, mp >300 °C; ν_{max}(KBr)/cm^{–1} 1611 (COO[–]) (Calc. for C₄₁H₅₁O₁₃Eu: H, 5.69; Eu³⁺, 16.8. Found: H, 5.83; Eu³⁺, 15.3%[‡]).

† The C content of the Eu³⁺ complexes determined by elemental analysis was too low, probably due to the formation of very stable Eu³⁺ carbides (*T*_{dec} > 1800 °C). For **3·Eu³⁺** no satisfactory elemental analysis could be obtained.

‡ No satisfactory mass spectrum of the acyclic complex **2·Eu³⁺** could be obtained.

2,2'-(1,3-Dioxolan-2-ylmethyl)aminodiethanol (9). A solution of 2-bromomethyl-1,3-dioxolane (1.00 g, 9.66 mmol), diethanolamine (5.08 g, 48.3 mol) and a catalytic amount of KI was refluxed in CH₃CN (30 ml) for 3 days. After cooling the reaction mixture to room temperature, the salts were filtered off, and the organic solvent was evaporated. The residue was dissolved in CH₂Cl₂ and washed subsequently with brine (2×). The organic layer was separated and dried with Na₂SO₄. After evaporation of the solvent, a blank oil was obtained in 65% yield. δ_{H} 4.88 (t, 1 H, *J* 4.2, CH), 3.9–3.7 (m, 4 H, OCH₂^{diox}), 3.60 (br s, 2 H, OH), 3.6–3.5 (m, 4 H, OCH₂), 2.8–2.6 (m, 6 H, NCH₂); δ_{C} 103.1 (d, CH), 64.8 (t, OCH₂^{diox}), 59.6 (t, OCH₂), 57.7 (t, NCH₂), 57.0 (t, NCH₂^{chain}); *m/z* (EIMS) 191.1 (M⁺, calc. for C₈H₁₇NO₄: 191.1).

16-(1,3-Dioxolan-2-ylmethyl)-4,9,23-trimethyl-13,19-dioxo-16-azatetracyclo[19.3.1.1^{2,6}.1^{7,11}]heptacos-1(25),2,4,6(27),7,9,11(26),21,23-nonaene-25,26,27-triol (10). The macrocyclization was performed in the same way as described for **1**,¹ using a solution of dibromide **4** (4.55 g, 7.26 mmol) in THF (25 ml), a solution of diol **9** (1.53 g, 8.00 mmol) in THF (25 ml) and a suspension of NaH (1.27 g, 29 mmol) in THF (400 ml). The phenolic groups were deprotected by refluxing the crude product with Pd(PPh₃)₄ (0.74 g, 0.82 mmol) and Et₃N·HCOOH (4.04 g, 27.4 mmol) in a mixture of EtOH (100 ml) and water (20 ml) for 2 h. After cooling the resulting mixture to room temperature, most of the solvent was evaporated and the residue was dissolved in CH₂Cl₂. The organic layer was washed twice with brine and dried over MgSO₄. Purification was performed by flash column chromatography (MeOH:CHCl₃ = 2:98) and a slightly yellow solid was obtained in 18% yield, mp 201–203 °C. δ_{H} 7.16 (s, 4 H, ArH), 6.90 (s, 2 H, ArH), 6.32 (br s, 3 H, OH), 4.87 (t, 1 H, *J* 4.4, CH), 4.71 (br s, 4 H, ArCH₂O), 3.9–3.7 (m, 2 H, OCH₂^{diox}), 3.7–3.6 (m, 2 H, OCH₂^{diox}), 3.68 (t, 4 H, *J* 5.8, OCH₂), 2.89 (t, 4 H, *J* 5.8, NCH₂), 2.76 (d, 2 H, *J* 4.4, NCH₂^{chain}), 2.40 (s, 3 H, ArCH₃ⁱ), 2.31 (s, 6 H, ArCH₃^o); δ_{C} 151.1 (s, ArC–O^o), 149.1 (s, ArC–Oⁱ), 130.7–122.9 (ArC), 103.0 (d, CH), 71.4 (t, Ar–CH₂O), 68.2 (t, OCH₂), 64.7 (t, OCH₂^{diox}), 56.6 (t, NCH₂), 56.5 (t, NCH₂^{chain}), 20.9 (q, CH₃ⁱ), 20.6 (q, CH₃^o); *m/z* (FABMS) 536.4 [(M + H)⁺, calc. for C₃₁H₃₈NO₇: 536.3] (Calc. for C₃₁H₃₇NO₇: C, 69.51; H, 6.96; N, 2.61. Found: C, 69.64; H, 7.50; N, 2.58%).

16-(1,3-Dioxolan-2-ylmethyl)-25,26,27-tris(methoxycarbonylmethoxy)-4,9,23-trimethyl-13,19-dioxo-16-azatetracyclo[19.3.1.1^{2,6}.1^{7,11}]heptacos-1(25),2,4,6(27),7,9,11(26),21,23-nonaene (11). Triester **11** was obtained *via* the previously described procedure,¹ as the NaClO₄ complex, in quantitative yield, using triol **10** (0.40 g, 0.75 mmol), K₂CO₃ (1.03 g, 7.45 mmol), NaClO₄ (1.37 g, 11.2 mmol), methyl bromoacetate (0.28 ml, 3.01 mmol) and CH₃CN (25 ml). The slightly yellow foam was pure according to ¹H NMR spectroscopy. δ_{H} 7.28 (s, 2 H, ArHⁱ), 7.05 (d, 2 H, *J* 2.0, ArH^o), 7.01 (d, 2 H, *J* 2.0, ArH^o), 5.10 (t, 1 H, *J* 4.4, CH), 4.99 and 4.05 (AB-q, 4 H, *J* 9.9, ArCH₂O), 4.0–3.8 (m, 8 H, ArOCH₂^o, OCH₂ and OCH₂^{diox}), 3.8–3.7 (m, 2 H, OCH₂^{diox}), 3.62 (s, 6 H, OCH₃^o), 3.44 (s, 3 H, OCH₃ⁱ), 3.5–3.4 (m, 2 H, OCH₂), 3.0–2.9 (m, 6 H, NCH₂ and NCH₂^{chain}), 2.93 (s, 2 H, ArOCH₂ⁱ), 2.45 (s, 3 H, ArCH₃ⁱ), 2.27 (s, 6 H, ArCH₃^o); δ_{C} 169.8 (s, C=O^o), 169.1 (s, C=Oⁱ), 154.0 (s, ArC–O^o), 149.1 (s, ArC–Oⁱ), 137.1–129.2 (ArC), 100.1 (d, CH), 71.7 (t, Ar–CH₂O), 70.9 (t, ArO–CH₂^o), 67.9 (t, ArO–CH₂ⁱ), 67.7 (t, OCH₂), 64.8 (t, OCH₂^{diox}), 55.8 (t, NCH₂), 52.4 (q, OCH₃^o), 52.4 (t, OCH₃ⁱ), 49.8 (t, NCH₂^{chain}), 21.3 (q, CH₃ⁱ), 20.8 (q, CH₃^o); *m/z* (FABMS) 774.3 [(M + Na)⁺, calc. for C₄₀H₄₉NO₁₃: Na: 774.3], 700.3 [(M + Na – CH₂COOCH₃)⁺], 626.3 [(M + Na – 2 × CH₂COOCH₃)⁺].

16-(1,3-Dioxolan-2-ylmethyl)-25,26,27-tris(hydroxycarbonylmethoxy)-4,9,23-trimethyl-13,19-dioxo-16-azatetracyclo[19.3.1.1^{2,6}.1^{7,11}]heptacos-1(25),2,4,6(27),7,9,11(26),21,23-nonaene (12). Triacid **12** was synthesized as described for **8**, using triester **11** (0.25 g, 0.33 mmol), MeOH (20 ml), NaOMe [Na (40 mg, 1.7 mmol) and 5 ml of MeOH] (2×) and water (40 μl,

2.2 mmol) (2×). The product was obtained in almost quantitative yield as an off-white foam. ν_{max} (KBr)/cm⁻¹ 1749, 1718 (C=O); *m/z* (FABMS) 732.3 [(M + Na)⁺, calc. for C₃₇H₄₃NO₁₃: Na: 732.3], 710.3 [(M + H)⁺].

16-(1,3-Dioxolan-2-ylmethyl)-25,26,27-tris(carboxylatomethoxy)-4,9,23-trimethyl-13,19-dioxo-16-azatetracyclo[19.3.1.1^{2,6}.1^{7,11}]heptacos-1(25),2,4,6(27),7,9,11(26),21,23-nonaene europium(III) (3·Eu³⁺). The reaction was carried out using triacid **12** (0.80 g, 0.83 mmol) and Et₃N (0.34 ml, 2.47 mol) in MeOH (10 ml), and EuCl₃·6H₂O (0.34 g, 0.93 mmol) in MeOH (3 ml). The off-white solid **3·Eu³⁺** was obtained in quantitative yield, mp >300 °C; ν_{max} (KBr)/cm⁻¹ 1608 (COO⁻); *m/z* (FABMS/PEG200) 858.2 [(M + H)⁺, calc. for C₃₇H₄₁NO₁₃Eu: 858.2].

16-(1,3-Dioxolan-2-ylmethyl)-25,26,27-tris(carboxylatomethoxy)-4,9,23-trimethyl-13,19-dioxo-16-azatetracyclo[19.3.1.1^{2,6}.1^{7,11}]heptacos-1(25),2,4,6(27),7,9,11(26),21,23-nonaene neodymium(III) (3·Nd³⁺). The reaction was carried out using triacid **12** (42 mg, 59 μmol) and Et₃N (25 μl, 0.18 mmol) in MeOH (2 ml), and Nd(NO₃)₃·5H₂O (31 mg, 71 μmol) in MeOH (1 ml). The off-white solid **3·Nd³⁺** was obtained in quantitative yield, mp >300 °C; ν_{max} (KBr)/cm⁻¹ 1608 (COO⁻); *m/z* (FABMS) 849.2 [(M + H)⁺, calc. for C₃₇H₄₁NO₁₃Nd: 849.2].

Molecular modelling

The protocol for molecular mechanics and dynamics is described by van Veggel and Reinhoudt.⁷

Photophysical studies

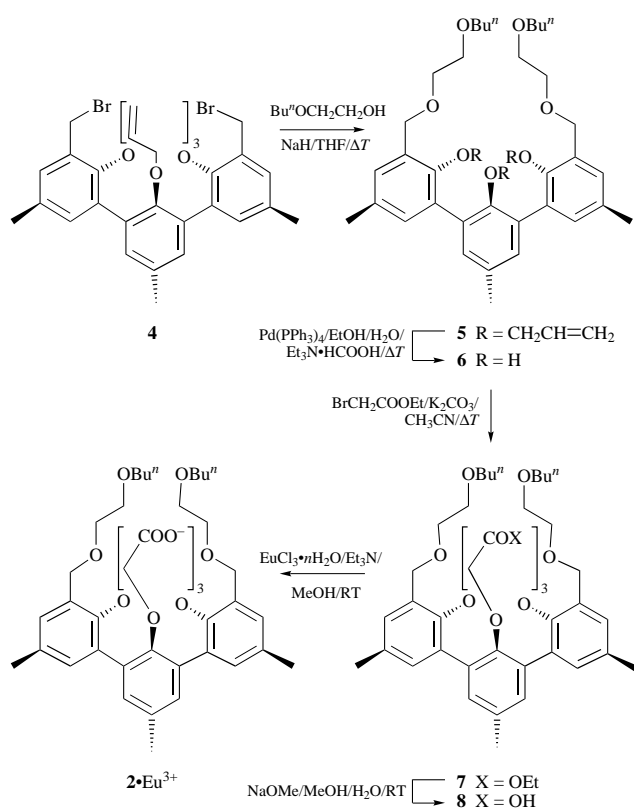
Steady-state luminescence measurements were performed with a PTI (Photon Technology International) Alphascan spectrofluorimeter. For excitation, a 75 W quartz–tungsten–halogen lamp followed by a SPEX 1680 double monochromator was used. A PTI 0.25 m single monochromator was used for separation of the emitted light, which was detected at an angle of 90°. The signal from the Hamamatsu R928 photomultiplier was fed to a photon counting interface. For the 'slow' time-resolved measurements in the phase resolved mode, the excitation beam was modulated in intensity at a frequency of 30–400 Hz by means of an optical chopper. The modulated luminescence signal was subsequently analyzed with a Stanford Research SR530 lock-in amplifier. The frequency dependence of the phase shift and demodulation of the luminescence signal was fitted to well-known expressions applied for phase-resolved luminescence data.⁸ For fast time-resolved luminescence measurements, an Edinburgh Analytical Instruments LP900 system was used, which consisted of a pulsed Xe lamp followed by a 0.25 m monochromator for excitation and another 0.25 m monochromator, used for the separation of light, positioned at an angle of 90° with respect to the first one. The near-IR photons were transformed into electric signals by means of a NorthCoast EO817P liquid nitrogen cooled germanium detector and fed to a Tektronix fast digital oscilloscope. The emission quantum yields were evaluated with a Perkin-Elmer 650-40 following the method described by Haas and Stein,⁹ using Ru(bpy)₃²⁺ ($\phi = 0.028$ in aerated water¹⁰) as a standard (experimental error ≈ 10%).

Because of the sensitivity of the Eu³⁺ luminescence lifetimes and intensities to the water content of the solutions, methanol was dried over molecular sieves (3 Å) prior to use and the lifetimes and luminescence spectra were recorded using freshly prepared samples.

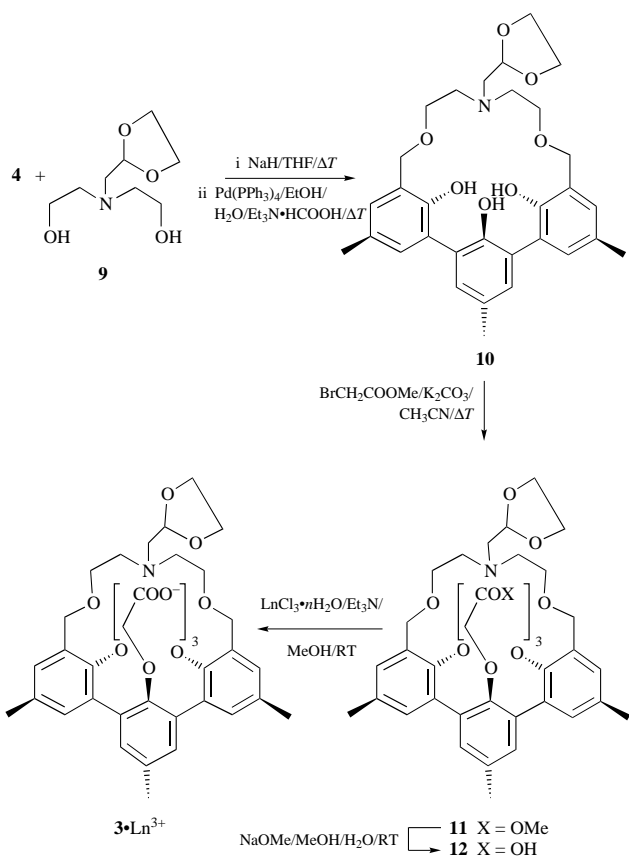
Results and discussion

Synthesis

The lanthanide ion complexes **2·Eu³⁺** (Scheme 1), **3·Eu³⁺** and **3·Nd³⁺** (Scheme 2) were synthesized starting from the bis-(bromomethyl)terphenyl **4**.¹ The alkylation reaction of *n*-butoxyethanol with bis(bromomethyl)terphenyl **4** in refluxing



Scheme 1



Scheme 2

THF, in the presence of NaH as a base, gave **5** in quantitative yield. The ^1H NMR spectrum shows a singlet for the benzylic protons at 4.64 ppm. The mass of **5** (m/z 700.8, FAB mass spectrometry) corresponds to the calculated value for M^+ ($\text{C}_{44}\text{H}_{60}\text{O}_7$: 700.4). The hydroxy groups in **5** were deprotected

with $\text{Pd}(\text{PPh}_3)_4$ and $\text{Et}_3\text{N}\cdot\text{HCOOH}$ in a refluxing mixture of ethanol and water (v/v 5:1)¹¹ giving **6** in 86% yield. Triester **7** was synthesized by alkylation of the hydroxy groups with ethyl bromoacetate in acetonitrile using K_2CO_3 as a base. After purification by column chromatography **7** was obtained in 82% yield; the ^1H NMR spectrum shows two broad singlets at 4.25 and 4.12 ppm for the methylene hydrogens of the outer and inner pendant arms, respectively, and the FAB mass spectrum shows the highest peak at m/z 861.1 which is attributed to $(\text{M} + \text{Na})^+$ ($\text{C}_{47}\text{H}_{66}\text{O}_{13}\text{Na}$: 861.5). The base-catalyzed hydrolysis of **7** was carried out in methanol in the presence of $\text{NaOMe}\text{-H}_2\text{O}$ leading to triacid **8** in almost quantitative yield. The broad signal at 7.98 ppm in the ^1H NMR spectrum with a relative intensity of three hydrogens is attributed to the carboxylic acids and the highest peak in the FAB mass spectrum at m/z 777.0 is attributed to $(\text{M} + \text{Na})^+$ ($\text{C}_{41}\text{H}_{54}\text{O}_{13}\text{Na}$: 777.4). Complexation of Eu^{3+} was achieved by reaction of one equivalent of $\text{EuCl}_3\cdot 6\text{H}_2\text{O}$ with triacid **8** in methanol, in the presence of three equivalents of Et_3N as a base. The complex $2\cdot\text{Eu}^{3+}$ was isolated by evaporation of the solvent, followed by the addition of water and subsequent extraction with CH_2Cl_2 . Complete deprotonation is obvious from the peak in the IR spectrum at 1611 cm^{-1} , which is attributed to the COO^- stretching vibration.

Diol **9** was obtained in 65% yield by the alkylation of diethanolamine with 2-bromomethyl-1,3-dioxolane in refluxing acetonitrile in the presence of a catalytic amount of KI. The macrocyclization of **4** with **9** was achieved according to the procedure we published previously.¹ The ^1H NMR spectrum of the reaction product shows an AB system at 4.57 and 4.25 ppm, which is attributed to the benzylic hydrogen atoms of the cyclic structure, indicating that the macrocycle was formed. All efforts to purify the product were unsuccessful and therefore the hydroxy groups of the crude product were deprotected in the same way as for **6**. After purification by flash column chromatography, triol **10** was obtained in 18% yield. The ^1H NMR spectrum shows a broad singlet for the benzylic hydrogen atoms at 4.71 ppm, whereas the broad singlet at 6.32 ppm is attributed to the protons of the hydroxy groups. The FAB mass spectrum shows the highest peak at 536.4, which corresponds to the calculated value of $(\text{M} + \text{H})^+$. Triol **10** was alkylated with methyl bromoacetate in acetonitrile with K_2CO_3 as a base, followed by hydrolysis in methanol in the presence of $\text{NaOMe}\text{-H}_2\text{O}$ giving triacid **12**. Triacid **12** was complexed with one equivalent of the appropriate lanthanide salt in the presence of three equivalents of Et_3N as a base, analogous to $1\cdot\text{Eu}^{3+}$.¹ The complexes precipitated and were characterized by FAB mass spectrometry, showing the highest peak for $3\cdot\text{Eu}^{3+}$ at m/z 858.2 and for $3\cdot\text{Nd}^{3+}$ at m/z 849.2, which can both be attributed to $(\text{M} + \text{H})^+$ ($\text{C}_{37}\text{H}_{41}\text{NO}_{13}\text{Ln}$: 858.2 and 849.2, respectively). The corresponding peaks in the FAB mass spectra clearly show the lanthanide isotope pattern. Furthermore, the IR spectra of both complexes show the COO^- stretch vibration at 1608 cm^{-1} .

Molecular modelling

The structures of the acyclic and the dioxolane containing Eu^{3+} complexes $2\cdot\text{Eu}^{3+}$ and $3\cdot\text{Eu}^{3+}$ were minimized in the gas phase and subjected to molecular dynamics simulations in a cubic OPLS box of methanol.⁷ These calculations show that the acyclic ligand **2** leaves apparently more space in the first coordination sphere of the Eu^{3+} ion [Fig. 1(a)] compared to the macrocyclic ligand **1**, leading to the coordination of two molecules of methanol to $2\cdot\text{Eu}^{3+}$ compared to one in $1\cdot\text{Eu}^{3+}$.¹ Despite the coordination of one of the oxygen atoms of the dioxolane group to the Eu^{3+} ion in $3\cdot\text{Eu}^{3+}$, this ion can still accommodate one molecule of methanol in its first coordination sphere [Fig. 1(b)].

Photophysical studies

The photophysical properties of Eu^{3+} complexed by the two new organic ligands **2** and **3** were studied in the same way as reported for $1\cdot\text{Eu}^{3+}$.¹ The excitation spectrum of $2\cdot\text{Eu}^{3+}$

together with that of $1 \cdot \text{Eu}^{3+}$ is depicted in Fig. 2(a) showing a stronger luminescence over the entire wavelength region of the spectrum for $2 \cdot \text{Eu}^{3+}$ compared to the spectrum for $1 \cdot \text{Eu}^{3+}$. At 287 nm the difference in intensity is approximately a factor of six. This may be due to a difference in the energy of the triplet states of the acyclic ligand **2** and the cyclic ligand **1**, leading to a more efficient energy transfer from the ligand **2** to the Eu^{3+} ion. § The absorption of ligand **2** is only 1.3 times higher than the absorption of ligand **1** and consequently this cannot be the only reason for the large difference in luminescence.

The emission spectrum of $2 \cdot \text{Eu}^{3+}$ in $[\text{D}_4]\text{methanol}$ after excitation at 287 nm shows the typical Eu^{3+} luminescence [Fig. 2(b)];⁵ for comparison the emission spectrum of $1 \cdot \text{Eu}^{3+}$ is also shown in Fig. 2(b). After ligand-mediated excitation, the luminescence intensity of the acyclic complex $2 \cdot \text{Eu}^{3+}$ is a factor of nine larger than that of $1 \cdot \text{Eu}^{3+}$, which can be explained by the relatively efficient energy transfer in $2 \cdot \text{Eu}^{3+}$. The luminescence quantum yield (ϕ_{lum}) can be expressed by eqn. (1).^{4,5c}

$$\phi_{\text{lum}} = \phi_{\text{isc}} \phi_{\text{et}} k_{\text{rad}} \tau \quad (1)$$

In eqn. (1), ϕ_{isc} is the efficiency of intersystem crossing within the chromophoric group, which is assumed to be similar for both complexes, ¶ ϕ_{et} is the efficiency of the ligand-to-metal energy transfer, k_{rad} is the radiative rate constant, which is assumed to be the same for all Eu^{3+} complexes and τ is the

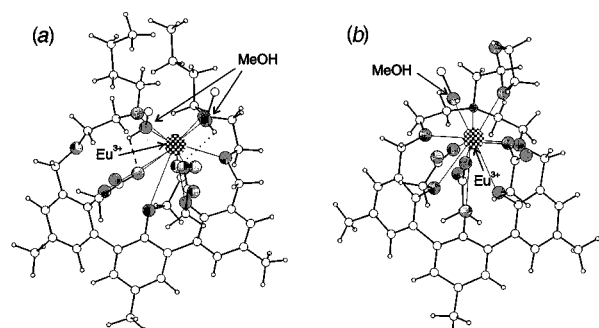


Fig. 1 Typical structures during the MD calculations (front view) of (a) $2 \cdot \text{Eu}^{3+}$ and (b) $1 \cdot \text{Eu}^{3+}$. The dotted circle represents the Eu^{3+} ion and the grey circles the heteroatoms.

§ The energy transfer efficiency is increasing with a shorter distance between the aromatic system and Eu^{3+} ($k_{\text{et}} \propto R^{-6}$ or e^{-R}); molecular modelling indicated that this distance is larger in $2 \cdot \text{Eu}^{3+}$ than in $1 \cdot \text{Eu}^{3+}$, and can thus not contribute to the more efficient energy transfer.

¶ Since the rate of intersystem crossing is much higher than the rate of energy transfer: $k_{\text{isc}} \gg k_{\text{et}}$.

observed luminescence lifetime. Hence, the luminescence intensity is mainly affected by τ and/or ϕ_{et} . The significantly larger increase in ϕ_{lum} compared to the increase in τ (Table 1) is consequently an effect of the more efficient energy transfer from the ligand to the Eu^{3+} ion. The quantum yield of $2 \cdot \text{Eu}^{3+}$ in $[\text{D}_4]\text{methanol}$ was determined to be 0.022, whereas in ordinary methanol this quantity is lowered to 0.004 due to solvent quenching. It was not possible to determine the quantum yield for $1 \cdot \text{Eu}^{3+}$, because the luminescence signal is too weak. The shape of the peak at 614 nm in the emission spectra of $1 \cdot \text{Eu}^{3+}$ and $2 \cdot \text{Eu}^{3+}$ is only slightly different, and moreover, the ratio between the intensity of the ${}^5\text{D}_0 \rightarrow {}^7\text{F}_1$ transition (at 580 nm) and the intensity of the hypersensitive ${}^5\text{D}_0 \rightarrow {}^7\text{F}_2$ transition (at 620 nm) is approximately equal. This implies that the symmetry around the Eu^{3+} ion, induced by the ligands and the solvent, is nearly constant, and therefore it is legitimate to compare the luminescence properties of the Eu^{3+} complexes notwithstanding variations in the ligand structure.¹²

The luminescence lifetime (Table 1) of $2 \cdot \text{Eu}^{3+}$ in methanol is as long as for $1 \cdot \text{Eu}^{3+}$, whereas the lifetimes of $2 \cdot \text{Eu}^{3+}$ in $[\text{D}_4]\text{methanol}$ and $[\text{D}_4]\text{methanol}$ are almost double. Using 'Horrocks equation':¹³ $n = 2.1(\tau_{\text{CH}_3\text{OH}}^{-1} - \tau_{\text{CD}_3\text{OD}}^{-1})$ to estimate the number of coordinating O–H oscillators n in the first coordination sphere of the Eu^{3+} ion leads to 1.9 ± 0.5 coordinating methanol molecules in $2 \cdot \text{Eu}^{3+}$ compared to $(0.9 - 1.2 \pm 0.5)$ in $1 \cdot \text{Eu}^{3+}$. This number was also determined from the radial distribution function of the molecular dynamics simulations, leading to 2.0 coordinating solvent molecules. This indicates that the shielding of the Eu^{3+} ion is decreased in the acyclic complex relative to the macrocyclic complex. Upon solvent deuteration the lifetime of $2 \cdot \text{Eu}^{3+}$ is increased by a factor of 2.8 compared to a factor of 1.5 for $1 \cdot \text{Eu}^{3+}$. This is also indicative of a higher rate constant for quenching by the O–H modes, as a result of the larger number of coordinating solvent molecules to the Eu^{3+} ions in $2 \cdot \text{Eu}^{3+}$ (Table 1). This rate constant is approximately double for $2 \cdot \text{Eu}^{3+}$ relative to $1 \cdot \text{Eu}^{3+}$. On the other hand, quenching by the acyclic ligand is not very efficient as can be concluded from the long luminescence lifetime of 2.41 ms in $[\text{D}_4]\text{methanol}$ compared to 2.53 ms for free Eu^{3+} ions in this solvent ($k_{\text{C-H}}^{\text{lig}} = 0.02 \text{ ms}^{-1}$).¹ This can be attributed to the relatively large distance between the high-energy vibrational modes of the acyclic ligand and the Eu^{3+} ion. On the other hand, quenching by the high-energy vibrational C–H modes of the macrocyclic complex $1 \cdot \text{Eu}^{3+}$ is of the same order of magnitude as quenching by one solvent molecule.¹ The luminescence lifetime of $2 \cdot \text{Eu}^{3+}$ in $[\text{D}_4]\text{methanol}$ is further increased by a factor of 1.2 due to the absence of the quenching C–H modes of the solvent. The rate constants for non-radiative decay *via* the O–H groups of the solvent, and the C–H vibrations of the solvent, and the C–H groups of the organic

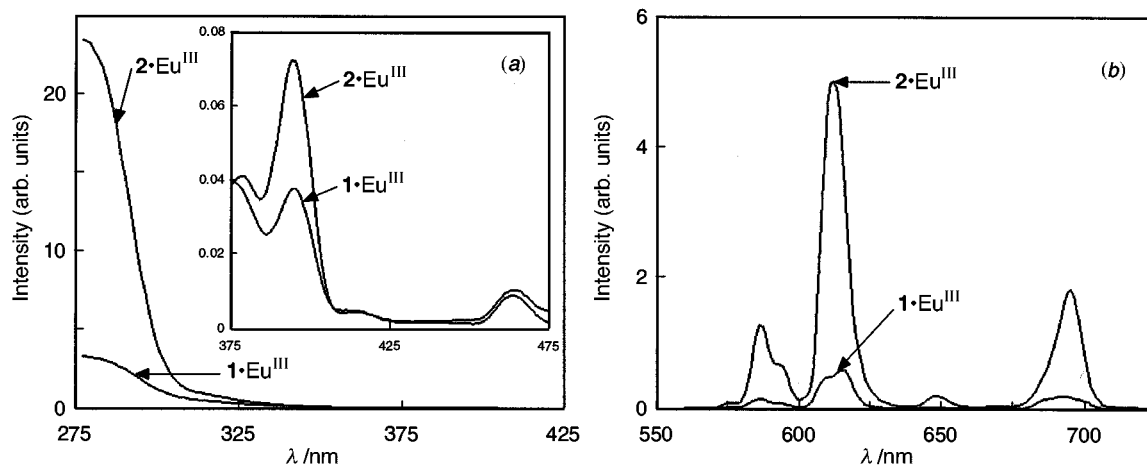


Fig. 2 (a) Excitation spectra detected at 617 nm and (b) emission spectra after excitation at 287 nm of 10^{-4} M solutions of $1 \cdot \text{Eu}^{3+}$ and $2 \cdot \text{Eu}^{3+}$ in $[\text{D}_4]\text{methanol}$

Table 1 Luminescence lifetimes (in ms) of 10^{-4} M methanol solutions of $1\cdot\text{Eu}^{3+}$, $2\cdot\text{Eu}^{3+}$ and $3\cdot\text{Eu}^{3+}$, the number of coordinating methanol molecules calculated from the luminescence lifetimes and by MD simulations and the calculated rate constants (in ms^{-1}) of the various quenching mechanisms

	$\tau_{\text{CH}_3\text{OH}}$	$\tau_{\text{CH}_3\text{OD}}$	$\tau_{\text{CD}_3\text{OD}}$	n^a	MD ^b	$k_{\text{O-H}}^c$	$k_{\text{C-H}}^{\text{solv } d}$	$k_{\text{C-H}}^{\text{lig } e}$
$2\cdot\text{Eu}^{3+}$	0.72	2.05	2.41	1.9	2.0	0.90	0.07	0.02
$3\cdot\text{Eu}^{3+}$	1.42	1.53	1.61	0.1	0.8	0.05	0.03	0.23
$1\cdot\text{Eu}^{3+}$	0.75	1.17	1.33	1.0	0.9	0.48	0.10	0.36

^a ± 0.5 , calculated from: $n = 2.1(\tau_{\text{CH}_3\text{OH}}^{-1} - \tau_{\text{CH}_3\text{OD}}^{-1})$. ^b The radial distribution function (RDF) can be calculated from the production phase, and the integrated area of the peak around 2.3 Å gives the number of coordinating solvent molecules. ^c $k_{\text{O-H}} = \tau_{\text{CH}_3\text{OH}}^{-1} - \tau_{\text{CH}_3\text{OD}}^{-1}$. ^d $k_{\text{C-H}}^{\text{solv}} = \tau_{\text{CH}_3\text{OD}}^{-1} - \tau_{\text{CD}_3\text{OD}}^{-1}$. ^e $k_{\text{C-H}}^{\text{lig}} = (\tau_{\text{complex}}^{-1} - \tau_{\text{EuCl}_3}^{-1})_{\text{CD}_3\text{OD}}$.

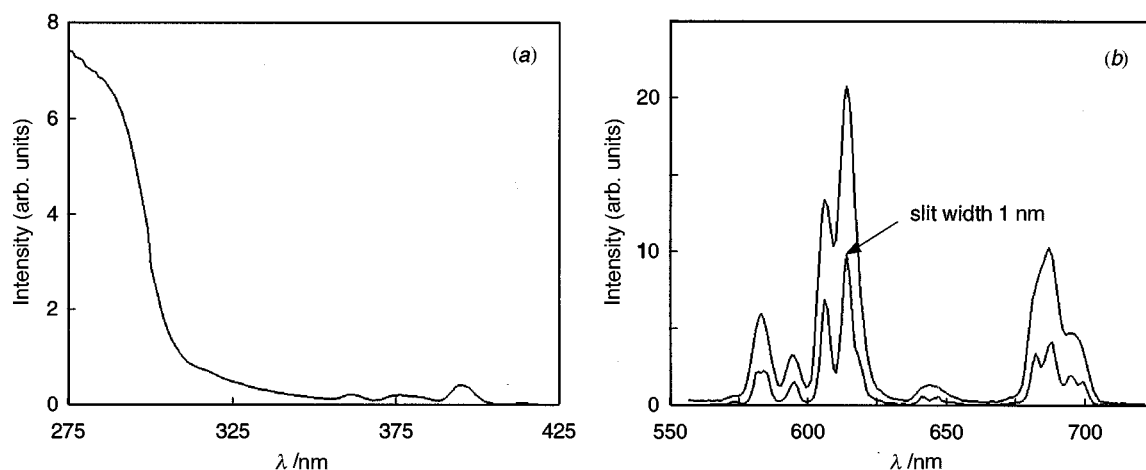


Fig. 3 (a) Excitation spectrum detected at 614 nm and (b) emission spectra after excitation at 287 nm of a 10^{-4} M solution of $3\cdot\text{Eu}^{3+}$ in $[\text{²H}_4]\text{methanol}$

ligand || were calculated by the equations given in Table 1. These values clearly show that quenching by the O–H groups of the solvent is strongly dominating over quenching by both types of C–H modes.

Preorganization¹⁴ of the encapsulating organic ligand seems to be important for its ability to shield lanthanide ions as was concluded from the decreased shielding in $2\cdot\text{Eu}^{3+}$ relative to $1\cdot\text{Eu}^{3+}$. Therefore, we introduced an extra coordination site in the preorganized ligand in the form of a dioxolane group in $3\cdot\text{Eu}^{3+}$, and investigated its luminescence properties by the same type of photophysical studies. The excitation spectrum of a 10^{-4} M solution of $3\cdot\text{Eu}^{3+}$ in $[\text{²H}_4]\text{methanol}$, depicted in Fig. 3(a), closely resembles the excitation spectrum of $1\cdot\text{Eu}^{3+}$, clearly showing the Eu^{3+} excitation band at 393 nm, whereas the emission spectrum [Fig. 3(b)] shows the typical Eu^{3+} luminescence.⁵ In order to improve the splitting of the ${}^5\text{D}_0 \rightarrow {}^7\text{F}_2$ emission band, the slit widths were narrowed to 1 nm [Fig. 3(b)]. With these narrow slit widths, the non-degenerate ${}^5\text{D}_0 \rightarrow {}^7\text{F}_0$ transition is split into two bands, indicating the coexistence of two different Eu^{3+} ions that experience a different symmetry from the ligand. Comparison of the emission spectra depicted in Figs. 2(b) and 3(b) show that the $({}^3\text{D}_0 \rightarrow {}^7\text{F}_2)/({}^3\text{D}_0 \rightarrow {}^7\text{F}_1)$ ratio is different for $3\cdot\text{Eu}^{3+}$, indicating that a direct comparison with $1\cdot\text{Eu}^{3+}$ and $2\cdot\text{Eu}^{3+}$ is not possible.¹² The difference in symmetry might be induced by the coordination of a molecule of methanol or water into the first coordination sphere and the two ${}^5\text{D}_0 \rightarrow {}^7\text{F}_0$ transitions might originate from $3\cdot\text{Eu}^{3+}$ with and without an additional solvent molecule coordinating to the Eu^{3+} ion.

The luminescence lifetimes of $3\cdot\text{Eu}^{3+}$ were determined for 10^{-4} M methanol solutions, after excitation *via* the ligand at 300

nm (Table 1). These lifetimes are relatively high, especially the lifetime of 1.42 ms for the all-hydrogen complex $3\cdot\text{Eu}^{3+}$ dissolved in non-deuterated methanol. The lifetime is only slightly increased (by a factor of 1.1) upon deuteration of the solvent, which indicates that the effective quenching modes of the solvent molecules are not present in the first coordination sphere of the Eu^{3+} . This is further established by 'Horrocks equation':¹³ $n = 2.1(\tau_{\text{CH}_3\text{OH}}^{-1} - \tau_{\text{CH}_3\text{OD}}^{-1})$, giving an estimated number of 0.1 ± 0.5 O–H oscillators. It is assumed that quenching of the luminescent excited state is mainly the result of solvent molecules present in the second coordination sphere around the Eu^{3+} ion that occasionally penetrate the first coordination sphere of the ion.** Consequently, the presence of an extra donor atom, which is capable of coordinating to the Eu^{3+} ion (according to molecular modelling), increases the luminescence lifetime by a factor of 1.9 in non-deuterated methanol compared to $1\cdot\text{Eu}^{3+}$, as the result of the higher degree of shielding. The RDF calculated for $3\cdot\text{Eu}^{3+}$ from the MD calculations is 0.8 which is higher than the experimentally determined value of 0.1 ± 0.5 . A reason for the discrepancy between the values for the number of coordinating solvent molecules lies in the use of a Ca^{2+} ion that is given the charge 3^+ as a model for Eu^{3+} . The ionic radius of Ca^{2+} is slightly larger than the radius of Eu^{3+} , 0.99 Å compared to 0.95 Å, respectively.††

The rate constants for quenching *via* the different pathways that are operative are reported in Table 1. The rate constant for quenching by the organic ligand is the most important one

** The MD calculations were performed with a production phase of 500 ps, which is too short to observe this type of exchange.

†† Quenching of the luminescence of $3\cdot\text{Nd}^{3+}$ by coordinating methanol molecules is more pronounced (*vide infra*). The ionic radius of Nd^{3+} is 0.995 Å, which is almost equal to the radius of Ca^{2+} . However, molecular dynamics in which the radius of the Eu^{3+} ion is reduced by 4%, also showed the coordination of one methanol molecule. In this case the penetration of the first coordination sphere occurs at 32 ps whereas the methanol already coordinates to the larger Eu^{3+} ion at the beginning of the production phase.

|| In this case it is not possible to calculate the rate constant for quenching by the ligand from a partially-deuterated and a non-deuterated complex. Therefore, the lifetime of EuCl_3 in $[\text{²H}_4]\text{methanol}$ was used as the maximum lifetime and it is assumed that quenching takes place mainly by the high-energy vibrational C–H modes of the ligand.

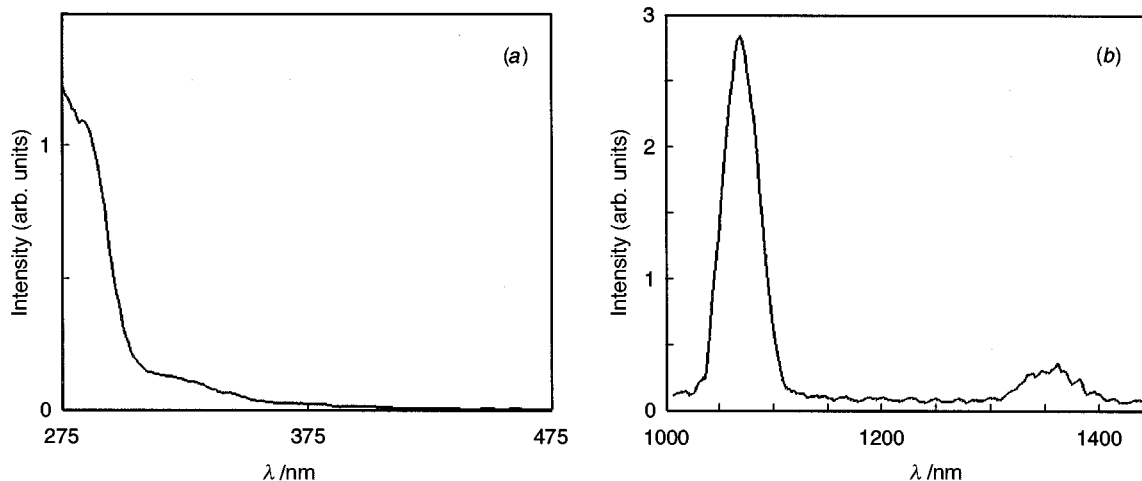


Fig. 4 (a) Excitation spectrum detected at 1060 nm and (b) emission spectra after excitation at 300 nm of a 10^{-4} M solution of $3 \cdot \text{Nd}^{3+}$ in $[\text{}^2\text{H}_4]\text{methanol}$

Table 2 Luminescence lifetimes of 10^{-4} M methanol solutions of $3 \cdot \text{Nd}^{3+}$

	$\tau/\mu\text{s}$
CH_3OH	$\leq 0.20^a$
CH_3OD	0.39
CD_3OD	0.52

^a Equal to the response time of the detector.

in $3 \cdot \text{Eu}^{3+}$. Compared to $1 \cdot \text{Eu}^{3+}$, this rate constant is slightly decreased from 0.36 ms^{-1} to 0.23 ms^{-1} , which might be an effect of small structural changes in the organic ligand. The dominating ligand quenching is a result of the very small number of solvent molecules in the first coordination sphere of the Eu^{3+} ion, and implies that the luminescent excited state of the Eu^{3+} ion may live even longer upon deuteration of $3 \cdot \text{Eu}^{3+}$.¹⁻³

Because of the interesting emission bands of Nd^{3+} in the near-IR part of the electromagnetic spectrum, *i.e.* at 1060 and 1350 nm, luminescence studies were performed with 10^{-4} M methanol solutions of $3 \cdot \text{Nd}^{3+}$. The excitation spectrum, depicted in Fig. 4(a), shows that the luminescence intensity is profoundly increased upon ligand-mediated excitation of Nd^{3+} . The luminescence lifetimes in different types of methanol are reported in Table 2, and clearly show the quenching effect of the solvent on the luminescence lifetime. Both O–H and C–H modes of the solvent participate in efficient quenching due to a smaller energy gap between the luminescent level and a lower-lying state compared to Eu^{3+} . The results also indicate that Nd^{3+} leaves apparently more space for solvent coordination relative to the analogous Eu^{3+} complex, which might be the result of the larger ionic radius of Nd^{3+} (0.995 \AA compared to Eu^{3+} 0.95 \AA). In addition, C–D and O–D vibrations of the solvent are relatively efficient in quenching the luminescent state of Nd^{3+} .¹⁵ This is the effect of the magnitude of the energy gap between the luminescent, ${}^4\text{F}_{3/2}$, state of Nd^{3+} and the lower-lying ${}^4\text{I}_{15/2}$ level ($\Delta E_{\text{Nd}^{3+}} \approx 5300 \text{ cm}^{-1}$), which is more or less resonant with the first overtone of the O–D vibration ($\nu_{\text{O-D}} \approx 2400 \text{ cm}^{-1}$).¹⁶ Therefore, it is not possible to discriminate between the several quenching processes and to calculate the rate constants, as was possible for the Eu^{3+} complexes.

Conclusions

Both complexes $2 \cdot \text{Eu}^{3+}$ and $3 \cdot \text{Eu}^{3+}$ show the typical Eu^{3+} luminescence and both have relatively long luminescence lifetimes in methanol solutions compared to $1 \cdot \text{Eu}^{3+}$. The reason for the long lifetime of $2 \cdot \text{Eu}^{3+}$ is the very low efficiency of quenching

by the organic ligand, although the degree of shielding is significantly decreased leading to the coordination of two strongly quenching methanol molecules in the first coordination sphere of the Eu^{3+} ion in $2 \cdot \text{Eu}^{3+}$. Consequently, the O–H vibrations of the solvent form the main quenching pathway. Moreover, the energy transfer from the organic ligand to the Eu^{3+} ion is far more efficient in the more flexible, acyclic, complex ($2 \cdot \text{Eu}^{3+}$), which is thus the better sensitizer.

The long luminescence lifetime of $3 \cdot \text{Eu}^{3+}$ is the result of the high degree of shielding of the Eu^{3+} ion; the number of solvent molecules present in the first coordination sphere of the Eu^{3+} ion is minimal, due to the additional coordination of an oxygen atom of the dioxolane group to Eu^{3+} . Due to this improved shielding, quenching *via* the organic ligand becomes dominant, whereas the solvent molecules have only minor effects on the luminescence lifetimes. Near-IR emission at 1060 and 1350 nm was detected for $3 \cdot \text{Nd}^{3+}$ after ligand-mediated excitation. Lifetime measurements proved that solvent molecules do coordinate in the first coordination sphere of the larger ion Nd^{3+} , when it is complexed by 3.

Acknowledgements

Akzo Nobel Central Research b.v. Arnhem is gratefully acknowledged for financial support.

References

- M. P. Oude Wolbers, F. C. J. M. van Veggel, B. H. M. Snellink-Ruël, J. W. Hofstraat, F. A. J. Geurts and D. N. Reinhoudt, *J. Am. Chem. Soc.*, 1997, **119**, 138.
- R. S. Dickins, D. Parker, A. S. de Sousa and J. A. G. Williams, *J. Chem. Soc., Chem. Commun.*, 1996, 697.
- I. Hemmilä, V.-M. Mikkala and H. Takalo, *J. Fluorescence*, 1995, **5**, 159.
- F. J. Steemers, W. Verboom, D. N. Reinhoudt, E. van der Tol and J. W. Verhoeven, *J. Am. Chem. Soc.*, 1995, **117**, 9408.
- (a) W. DeW. Horrocks, Jr. and M. Albin, *Proc. Inorg. Chem.*, 1984, **31**, 1; (b) B. Alpha, J.-M. Lehn and G. Mathis, *Angew. Chem., Int. Ed. Engl.*, 1987, **26**, 259; (c) N. Sabbatini, M. Guardigli and J.-M. Lehn, *Coord. Chem. Rev.*, 1993, **123**, 210; (d) D. Parker and J. A. G. Williams, *J. Chem. Soc., Dalton Trans.*, 1996, 3613; (e) D. M. Rudkevich, W. Verboom, E. van der Tol, C. J. van Staveren, F. M. Kaspersen, J. W. Verhoeven and D. N. Reinhoudt, *J. Chem. Soc., Perkin Trans. 2*, 1995, 131.
- The luminescence properties of the acyclic Nd^{3+} complex $2 \cdot \text{Nd}^{3+}$ will be described in a forthcoming paper, together with Pr^{3+} , Sm^{3+} , Tb^{3+} , Dy^{3+} and Yb^{3+} .
- The calculations were carried out following the protocol described by F. C. J. M. van Veggel and D. N. Reinhoudt, *Recl. Trav. Chim.*

- Pays-Bas*, 1995, **114**, 387, applying production phases of 250 and 500 ps for $2\cdot\text{Eu}^{3+}$ and $3\cdot\text{Eu}^{3+}$, respectively.
- 8 J. R. Lakowicz, *Principle of Fluorescence Spectroscopy*, Plenum Press, New York, 2nd edn., 1989.
- 9 Y. Haas and G. Stein, *J. Phys. Chem.*, 1971, **75**, 3668.
- 10 K. Nakamaru, *Bull. Chem. Soc. Jpn.*, 1982, **55**, 2697.
- 11 H. Hey and H.-J. Arpe, *Angew. Chem., Int. Ed. Engl.*, 1973, **12**, 928.
- 12 (a) A. F. Kirby, D. Foster and F. S. Richardson, *Chem. Phys. Lett.*, 1983, **95**, 507; (b) A. F. Kirby and F. S. Richardson, *J. Phys. Chem.*, 1983, **87**, 2544.
- 13 R. C. Holz, S. L. Klakamp, C. A. Chang and W. DeW. Horrocks, Jr., *Inorg. Chem.*, 1990, **29**, 2651.
- 14 K. E. Koenig, G. M. Lein, P. Stuckler, T. Kaneda and D. J. Cram, *J. Am. Chem. Soc.*, 1979, **101**, 3553.
- 15 The effects of ligand deuteration on the Nd^{3+} luminescence will be discussed in a forthcoming paper.
- 16 G. Stein and E. Würzberg, *J. Chem. Phys.*, 1975, **62**, 208.

Paper 7/03142D
Received 7th May 1997
Accepted 12th June 1997